Can ab initio theory explain the phenomenon of parity inversion in ^{11}Be?

Angelo Calci,[1,*] Petr Navrátil,[1,†] Robert Roth,[2] Jérémy Dohet-Eraly,[1] Sofia Quaglioni,[3] and Guillaume Hupin[4,5]

[1]*TRIUMF, 4004 Wesbrook Mall, Vancouver, British Columbia, V6T 2A3, Canada*
[2]*Institut für Kernphysik, Technische Universität Darmstadt, 64289 Darmstadt, Germany*
[3]*Lawrence Livermore National Laboratory, P.O. Box 808, L-414, Livermore, California 94551, USA*
[4]*Institut de Physique Nucléaire, Université Paris-Sud, IN2P3/CNRS, F-91406 Orsay Cedex, France*
[5]*CEA, DAM, DIF, F-91297 Arpajon, France*

(Dated: August 12, 2016)

The weakly-bound exotic ^{11}Be nucleus, famous for its ground-state parity inversion and distinct n+^{10}Be halo structure, is investigated from first principles using chiral two- and three-nucleon forces. An explicit treatment of continuum effects is found to be indispensable. We study the sensitivity of the ^{11}Be spectrum to the details of the three-nucleon force and demonstrate that only certain chiral interactions are capable of reproducing the parity inversion. With such interactions, the extremely large E1 transition between the bound states is reproduced. Our photo-disintegration calculations discriminate between conflicting experimental data and predict a distinct dip around the $3/2^-_1$ resonance energy. Finally, we predict low-lying $3/2^+$ and $9/2^+$ resonances that are not or not sufficiently measured in experiment.

Introduction. The theoretical understanding of exotic neutron-rich nuclei constitutes a tremendous challenge. These systems often cannot be explained by mean-field approaches and contradict the regular shell structure. The spectrum of ^{11}Be has some very peculiar features. The $1/2^+$ ground state (g.s.) is loosely bound by 502 keV with respect to the n+^{10}Be threshold and is separated by only 320 keV from its parity-inverted $1/2^-$ partner [1], which would be the expected g.s. in the standard shell-model picture of p-shell nuclei. Such parity inversion, already noticed by Talmi and Unna [2] in the early 1960s, is one of the best examples of disappearance of the $N = 8$ magic number with increasing neutron to proton ratio, N/Z. The next (n+n+^{9}Be) break-up threshold, appears at 7.31 MeV [3], such that the rich resonance structure at low energies is dominated by the n+^{10}Be dynamics. Peculiar is also the electric-dipole transition strength between the two bound states, which has attracted much attention since its first measurement in 1971 [4], and was remeasured in 1983 [5] and 2014 [6]. It is the strongest known transition between low-lying states, attributed to the halo character of ^{11}Be.

Pioneering investigations of ^{11}Be were performed with the *ab initio* no-core shell model (NCSM) [7] and the NCSM combined with the resonating group method (RGM) [8, 9] using realistic nucleon-nucleon (NN) forces. However, those calculations did not include three-nucleon (3N) interactions and were incomplete in the treatment of continuum effects or short-range correlations, respectively. Thus, the question remains if converged *ab initio* calculations can provide an accurate description of the ^{11}Be spectrum and reproduce the experimental ground state. In fact, we anticipate that an accurate description of this complex spectrum is sensitive to the details of the nuclear force [10]. In this paper, we report the first *ab initio* calculations that include both 3N and continuum effects using the no-core shell model with continuum (NCSMC) approach [11–13].

The nuclear interactions. Nowadays the most promising candidates of the nuclear forces are derived from chiral effective field theory (EFT), where NN, 3N and higher many-body interactions arise in a natural hierarchy [14–20]. In the following we investigate the most-commonly used chiral NN interaction obtained at N^{3}LO [21] augmented with a local 3N force at N^{2}LO with a cutoff of $\Lambda_{3N} = 500$ MeV that was initially introduced in Ref. [22] and constrained in Ref. [23]. To analyze the sensitivity of the ^{11}Be spectrum to the 3N force we modify the cutoff Λ_{3N} or switch off certain contributions by setting the corresponding low energy constants (LECs) to zero as described in Refs. [24, 25]. In addition to this family of interactions, we also employ a novel NN+3N interaction obtained at N^{2}LO, named N^{2}LO$_{\rm SAT}$, obtained from a simultaneous fit of NN and 3N contributions to scattering data and selected many-body observables [26–28].

Many-body approach. The general idea of the NCSMC is to represent the A-nucleon wave function as the generalized cluster expansion [11–13]

$$|\Psi_A^{J^\pi T}\rangle = \sum_\lambda c_\lambda^{J^\pi T} |A\lambda J^\pi T\rangle + \sum_\nu \int {\rm d}r r^2 \frac{\gamma_\nu^{J^\pi T}(r)}{r} \mathcal{A}_\nu |\Phi_{\nu r}^{J^\pi T}\rangle \,. \tag{1}$$

The first term consists of an expansion over the NCSM eigenstates of the compound system $|A\lambda J^\pi T\rangle$ (here ^{11}Be) indexed by λ. These states are well suited to cover the localized correlations of the A-body system, but are inappropriate to describe clustering and scattering properties. The latter properties are addressed by the second term corresponding to an expansion over the antisymmetrized NCSM/RGM channels $\mathcal{A}_\nu |\Phi_{\nu r}^{J^\pi T}\rangle$ [9], which describe the two clusters (here n+^{10}Be) in relative motion. Here r denotes the relative distance of the clusters and ν is a collective index for the relevant quantum numbers. The expansion coefficients $c_\lambda^{J^\pi T}$ and the continuous relative-motion amplitudes $\gamma_\nu^{J^\pi T}(r)$ are obtained as a solution of the generalized eigenvalue problem derived by representing the Schrödinger equation in the model space of expansion (1) as detailed in Refs. [9, 12, 13]. The resulting NCSMC equations are solved by the coupled-channel R-matrix method on a Lagrange mesh [29–31]. The resonance energies and widths are deduced from the complex poles of the

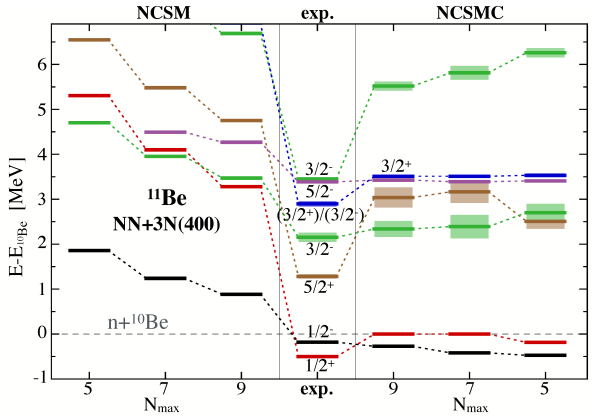

FIG. 1. (color online) Spectrum of ^{11}Be with respect to the n+^{10}Be threshold. The (IT-)NCSM (left) and NCSMC (right) calculations are carried out for different model space sizes ($N_{\max} = 5, 7, 9$). Light boxes of experimental and NCSMC spectra indicate resonance widths. Experimental energies taken from [1].

S-matrix, via the R-matrix approach extended to complex energies and momenta [32, 33].

The inclusion of the 3N force is computationally highly demanding and restricts the current application range of the NCSMC. For nuclei with $A > 5$ we rely on the formalism using uncoupled densities of Ref. [34]. The present NCSMC calculations are performed including the first three eigenstates ($0^+, 2^+_1, 2^+_2$) of the ^{10}Be target, entering the NCSM/RGM states in (1) and at least the first four negative- and three positive-parity eigenstates of ^{11}Be. Such eigenstates are obtained within the NCSM, except in the largest model spaces where, to reduce the dimension of the problem, we use the importance-truncated NCSM (IT-NCSM) [35, 36].

For accurate predictions of observables beyond excitation energies it is beneficial to loosen the first-principles paradigm and, in addition, introduce a phenomenology-inspired approach indicated by NCSMC-pheno that has been already used in Refs. [33, 37]. In this approach we adjust the ^{10}Be and ^{11}Be excitation energies of the NCSM eigenvectors entering expansion (1) to reproduce the experimental energies of the first low-lying states that impact in particular the photodisintegration process.

Analysis of spectroscopy. We start by using an interaction and parameter set established in numerous studies [24, 34, 38–40] and investigate the convergence with respect to the harmonic oscillator (HO) model-space size $N_{\max}$. Specifically we use the N^{3}LO NN and local N^{2}LO 3N interaction with $\Lambda_{3N} = 400$ MeV, indicated by NN+3N(400), the HO frequency $\hbar\Omega = 20$ MeV and an additional three-body truncation of the summed single-particle energies $e_1 + e_2 + e_3 \leq E_{3\max} = 14$. The interactions are softened via the similarity renormalization group (SRG) [41–43] at the three-body level up to a flow parameter of $\lambda_{\rm SRG} = 2.0\,\mathrm{fm}^{-1}$ ($\alpha = 0.0625\,\mathrm{fm}^4$) as described in Refs. [24, 44]. Note that, both the SRG induced and initial 3N forces are treated explicitly at all steps of the calculation.

The (IT-)NCSM spectrum is not converged at $N_{\max} = 9$. All states are unbound with respect to the n+^{10}Be threshold. The positive-parity states are extremely slowly converging and show a too high excitation energy compared to the negative-parity states. Once continuum effects are taken into account with the NCSMC the convergence improves drastically. However, the computed threshold energy of n+^{10}Be is not fully converged. At $N_{\max} = 9$ this energy is -58.4 MeV and gains 2.3, 6.2 MeV binding compared to the $N_{\max} = 7, 5$ model spaces, respectively. The extrapolated value of $-60.9(10)$ MeV is underbound with respect to the experimental energy of -64.976 MeV [3]. For the negative parity, the NCSMC achieves an overall reasonable theoretical description with the NN+3N(400) interaction, especially for the lowest three states. On the other hand, the $1/2^+$ state is barely bound and the parity inversion of the bound states is not reproduced. Similarly the $3/2^-_1$ and $5/2^+$ states are inverted compared to experiment. The $3/2^-_2$ excitation energy is about 2 MeV larger than the experimental one, which might be due to missing reaction channels at higher energies.

We first analyze the sensitivity of the spectrum to the 3N interaction in Fig. 2. The illustrated spectra are expected to show a similar convergence pattern as in the case of the NN+3N(400) interaction. From left to right we use exclusively the chiral NN interaction (including SRG induced 3N contributions), the 3N interaction with the 500 MeV cutoff, where contributions proportional to the c_3 LEC are suppressed ($c_3 = 0$), and the full 3N contributions using the cutoffs $\Lambda_{3N} = 500, 450, 400$, and 350 MeV. The omitted SRG-induced beyond-3N contributions are expected to impact the ^{11}Be spectrum only for the NN+3N(500) interaction, while the remaining spectra are anticipated to be unaffected [24, 44]. We find the c_3-term to cause the dominant 3N effects in the ^{11}Be spectrum. The 3N interactions generally increase the excitation energies of both $3/2^-$ resonances, corresponding to the increase in excitation energy of the 2^+ states in ^{10}Be. Neither the inversion of the $1/2^+$ and $1/2^-$ states, nor that of the $3/2^-_1$ and $5/2^+$ states can be explained by the adopted 3N force versions. Decreasing the 3N cutoff initially reduces the bound-state splitting, but below $\Lambda_{3N} = 400$ MeV the influence of the 3N interaction is reduced such that the spectra approach the pure NN result. On the contrary, the converged spectrum with the N^{2}LO$_{\rm SAT}$ interaction successfully achieves the parity inversions between the $3/2^-_1$ and $5/2^+$ resonances and, albeit marginally, for the bound states. The low-lying spectrum is significantly improved for the N^{2}LO$_{\rm SAT}$ interaction and agrees well with experiment, presumably due to the more accurate description of long-range properties caused by the fit of the interaction to radii of p-shell nuclei. On the other hand, the strongly overestimated splitting between the $3/2^-_2$ and $5/2^-$ states hints at deficiencies of this interaction, which might originate from a too large splitting of the $p_{1/2}$-$p_{3/2}$ sub shells.

In addition to the resonances observed in experiment all theoretical spectra predict a low-lying $9/2^+$ resonance suggested in Refs. [46, 47]. For the N^{2}LO$_{\rm SAT}$ interaction the res-

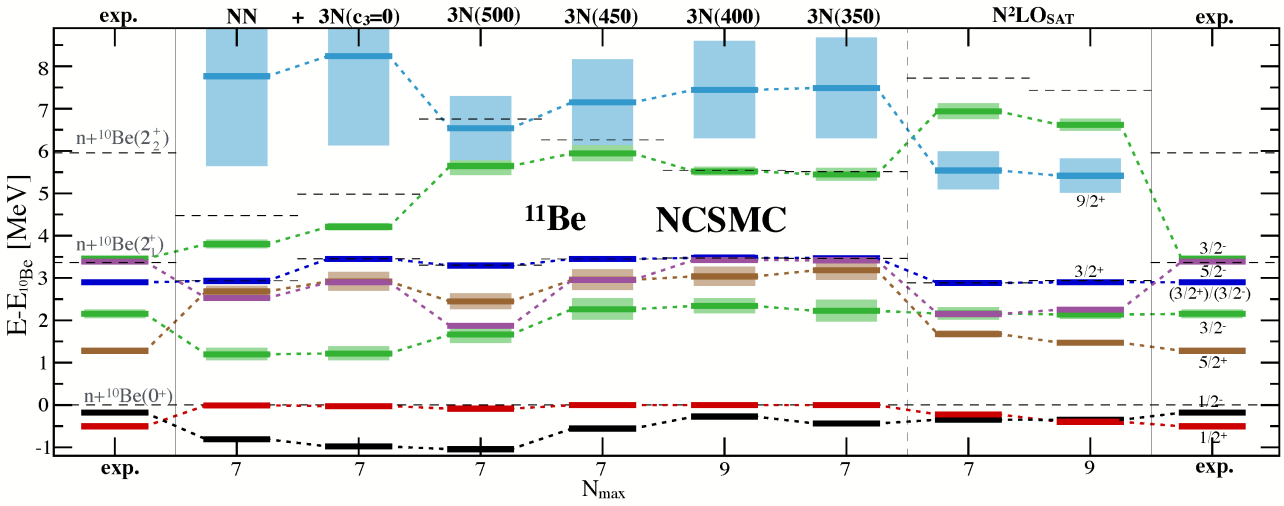

FIG. 2. (color online) NCSMC spectrum of ^{11}Be with respect to the n+^{10}Be threshold. Dashed black lines indicate energies of the ^{10}Be states. Light boxes indicate resonance width. Experimental energies taken from [1, 45].

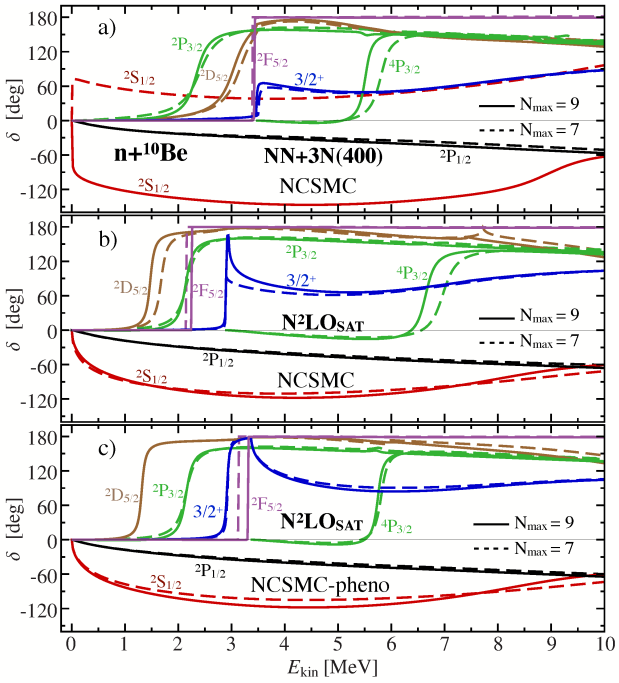

FIG. 3. (color online) The n+^{10}Be phase shifts as function of the kinetic energy in the center-of-mass frame. a) NCSMC phase shifts for the NN+3N(400) and b) the N^{2}LO$_{\rm SAT}$ interaction, as well as c) NCSMC-pheno phase shifts for the N^{2}LO$_{\rm SAT}$ interaction.

onance energy is close to the one predicted by the Gamow shell model [7], although our *ab initio* calculations predict a broader width. Another interesting property is the position of the $3/2^+$ resonance that is strongly influenced by the 2^+_1 state of ^{10}Be. For all theoretical calculations the energies of these correlated states are almost degenerate while in experiment the 2^+_1 state in ^{10}Be is about 470 keV above the tentative $3/2^+$ state and coincides with the $3/2^-_2$ and $5/2^-$ resonances.

J^π	NCSMC NN+3N(400) E	NCSMC NN+3N(400) Γ	NCSMC N^{2}LO$_{\rm SAT}$ E	NCSMC N^{2}LO$_{\rm SAT}$ Γ	NCSMC-pheno N^{2}LO$_{\rm SAT}$ E	NCSMC-pheno N^{2}LO$_{\rm SAT}$ Γ	exp. E	exp. Γ
$1/2^+$	-0.001	-	-0.40	-	-0.50	-	-0.50	-
$1/2^-$	-0.27	-	-0.35	-	-0.18	-	-0.18	-
$5/2^+$	3.03	0.44	1.47	0.12	1.31	0.10	1.28	0.1
$3/2^-_1$	2.34	0.35	2.14	0.21	2.15	0.19	2.15	0.21
$3/2^+$	3.48	-	2.90	0.014	2.92	0.06	2.898	0.122
$5/2^-$	3.43	0.001	2.25	0.0001	3.30	0.0002	3.3874	<0.008
$3/2^-_2$	5.52	0.20	6.62	0.29	5.72	0.19	3.45	0.01
$9/2^+$	7.44	2.30	5.42	0.80	5.59	0.62	-	-

TABLE I. Excitation spectrum of ^{11}Be with respect to the n+^{10}Be threshold. Energies and widths in MeV. NCSMC(-pheno) calculations are carried out at $N_{\rm max} = 9$.

Nuclear structure and reaction observables. The n+^{10}Be phase shifts are presented in Fig. 3 for the NCSMC and NCSMC-pheno approaches using two different interactions. The comparison of the phase shifts at $N_{\rm max} = 7$ and 9 confirms the good convergence with respect to the model space. The NN+3N(400) interaction predicts a barely bound $1/2^+$ state that appears to be a virtual state at $N_{\rm max} = 7$. The states observed in ^{11}Be are typically dominated by a single n+^{10}Be partial wave but the illustrated eigenphase shifts of the $3/2^+$ state consists of a superposition of the $^4S_{3/2}$ and $^2D_{3/2}$ partial waves. The parity of this resonance is experimentally not uniquely extracted [1], while all *ab initio* calculations concordantly predict a positive-parity state. In the case of the NN+3N(400) interaction, however, the fast variation of the $3/2^+$ phase shift near the n+^{10}Be(2^+_1) threshold does not correspond to a pole of the S-matrix. Thus, this state is not a resonance in the conventional sense and a width could not be extracted reliably. The bound-state energies as well as the resonance energies and widths are summarized in Tab. I. While the energies for the NCSMC-pheno approach are fitted to ex-

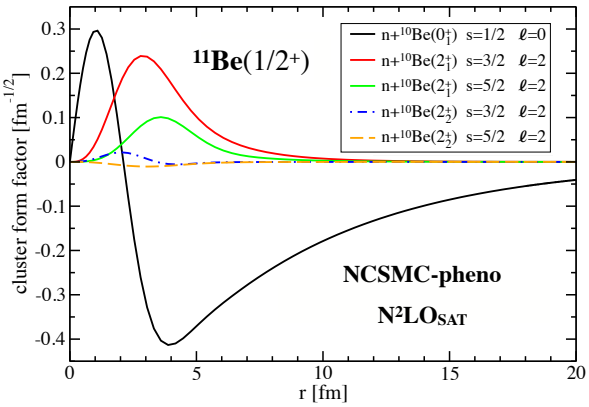

FIG. 4. (color online) Cluster form factor corresponding to the NCSMC-pheno calculation with the N^{2}LO$_{\rm SAT}$ interaction at $N_{\rm max}$ = 9. Note the coupling between the ^{10}Be target and neutron in the cluster state $|\Phi^{J\pi T}_{\nu,r}\rangle \sim [(|^{10}\mathrm{Be}: I^{\pi_1}_1 T_1\rangle\, |n: 1/2^+ 1/2\rangle)^{sT}\, Y_\ell(\hat{r})]^{J\pi T}$.

	NCSM	NCSMC	NCSMC-pheno	exp.
NN+3N(400)	0.0005	-	0.146	0.102(2) [6]
N^{2}LO$_{\rm SAT}$	0.0005	0.127	0.117	

TABLE II. Reduced transition probability B(E1: $1/2^- \rightarrow 1/2^+$) between ^{11}Be bound states in e^{2}fm^2.

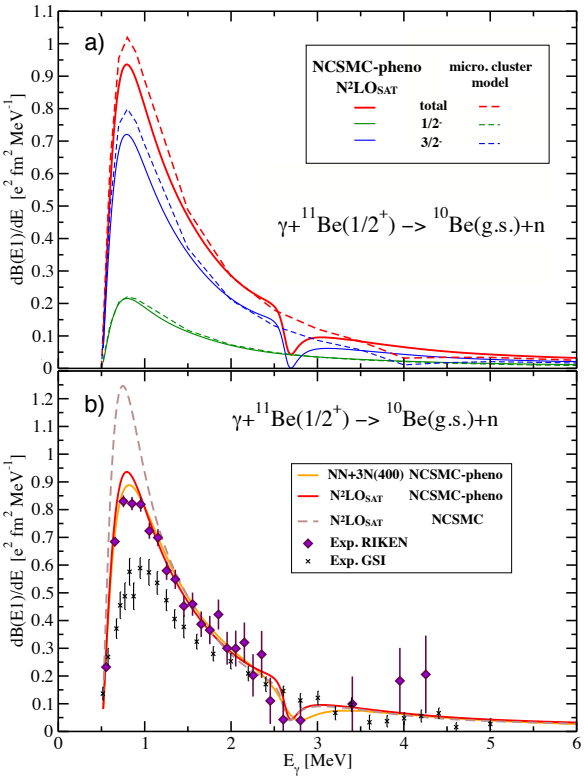

FIG. 5. (color online) Dipole strength distribution $dB(E1)/dE$ of the photodisintegration process as function of the photon energy. a) Partial wave contributions (thin lines) to the full dipole strength distribution (thick lines) obtained with the NCSMC-pheno using the N^{2}LO$_{\rm SAT}$ interaction (solid lines) compared to a microscopic cluster model [50] (dashed line). b) Dipole strength distribution for the N^{2}LO$_{\rm SAT}$ interaction with the NCSMC (brown) and NCSMC-pheno (red), as well as for the NN+3N(400) interaction with the NCSMC-pheno (orange) compared to the experimental measurements at GSI [51, 52] (black dots) and RIKEN [52–54] (violet dots).

periment the widths are predicted. The theoretical widths tend to overestimate the experimental ones but overall show a reasonable agreement, in particular for the N^{2}LO$_{\rm SAT}$ interaction. Experimentally only an upper bound could be determined for the $5/2^-$ resonance width and the N^{2}LO$_{\rm SAT}$ interaction predicts this resonance to be extremely narrow.

A physical intuition of the halo structure present in the ^{11}Be g.s. wave function, is provided by the cluster form factor in Fig. 4 given by $r \cdot \langle \Phi^{J\pi T}_{\nu,r} | \mathcal{A}_\nu | \Psi^{J\pi T}_A \rangle$ with $|\Psi^{J\pi T}_\nu\rangle$ and $|\Phi^{J\pi T}_{\nu,r}\rangle$ from (1). The corresponding spectroscopic factors are: S = 0.90 (S-wave) and S=0.16 (D-wave). The S-wave asymptotic normalization coefficient (ANC) is 0.786 fm$^{-1/2}$.

The B(E1) transitions are summarized in Tab. II. The NCSM calculations predict the wrong g.s. and underestimate the E1 strength by several orders of magnitude. For the NCSMC calculations with the NN+3N(400) interaction the $1/2^+$ state is very weakly bound leading to an unrealistic E1 transition. Within the NCSMC and NCSMC-pheno using the N^{2}LO$_{\rm SAT}$ interaction the strong E1 transition is successfully reproduced, albeit the latest measurement [6] is slightly overestimated. There might be small effects arising from a formally necessary SRG evolution of the operator. Works along these lines for ^{4}He suggest a slight reduction of the dipole strength, once the operator is consistently evolved [48, 49]. A similar effect would bring the calculated E1 transition in better agreement with the latest measurement [6].

Finally we study the photodisintegration of the ^{11}Be g.s. into n+^{10}Be in Fig. 5. We analyze the dipole strength distribution $dB(E1)/dE$ and the $1/2^-$ and $3/2^-$ contributions and compare the NCSMC and NCSMC-pheno approaches for the N^{2}LO$_{\rm SAT}$ and NN+3N(400) interactions to experiments and the microscopic cluster-model results of Ref. [50]. In all approaches, a peak of non-resonant nature (see Fig. 3) is present at about 800 keV above the n+^{10}Be threshold, particularly pronounced in the $3/2^-$ partial wave. The strong peak for the NCSMC with the N^{2}LO$_{\rm SAT}$ interaction is caused by the underestimated binding energy of $1/2^+$ state. The NCSMC-pheno prediction certainly discriminates between the two experimental data sets and agree well with the data from RIKEN [52–54]. A dip in the dipole strength distribution is present at about 2.7 MeV, due to the $3/2^-_1$ resonance. At this energy, the E1 matrix element between the ^{11}Be g.s. wave function and the $3/2^-$ partial wave of the n+^{10}Be scattering wave function cancels before changing its sign. Due to large uncertainties the experimental data neither confirm nor exclude such a dip. A similar feature, but much less pronounced, can be noticed in the microscopic cluster calculations around 4 MeV, which is close to the $3/2^-_1$ resonance energy (3.6 MeV) obtained with that model [50].

Conclusions. We have demonstrated that the inclusion of continuum effects is crucial for a description of the ^{11}Be sys-

tem. Moreover, the spectrum is extremely sensitive to the details of the nuclear NN+3N interactions and constitutes an important benchmark system for future forces. In particular, the parity inversion of the bound states could only be achieved by the N^2LO_{SAT} interaction that provides accurate predictions of nuclear radii and matter saturation properties [26, 27]. An interesting related endeavour is the investigation of the mirror system p+^{10}C. New experiments have been performed for the elastic scattering process [55] that will be analyzed with the NCSMC in a future work. Developments to combine the multi-reference normal-ordering [56] with the NCSMC approach are in progress, that will reduce the computational effort and make a variety of exotic physical systems accessible.

Acknowledgments. Prepared in part by LLNL under Contract DE-AC52-07NA27344. Supported by the U.S. Department of Energy, Office of Science, Office of Nuclear Physics, under Work Proposal No. SCW1158, by the NSERC Grants No. SAPIN-2016-00033 and by the Deutsche Forschungsgemeinschaft through SFB 1245. TRIUMF receives federal funding via a contribution agreement with the National Research Council of Canada. Computing support came from the LLNL institutional Computing Grand Challenge Program, from an INCITE Award on the Titan supercomputer of the Oak Ridge Leadership Computing Facility (OLCF) at ORNL, the LOEWE-CSC Frankfurt, the computing center of the TU Darmstadt (LICHTENBERG) and from Calcul Quebec and Compute Canada.

* calci@triumf.ca
† navratil@triumf.ca

[1] D. Tilley, J. Kelley, J. Godwin, D. Millener, J. Purcell, C. Sheu, and H. Weller, Nucl. Phys. A **745**, 155 (2004).
[2] I. Talmi and I. Unna, Phys. Rev. Lett. **4**, 469 (1960).
[3] M. Wang, G. Audi, A. H. Wapstra, F. G. Kondev, M. MacCormick, X. Xu, and B. Pfeiffer, Chinese Physics C **36**, 1603 (2012).
[4] S. S. Hanna, K. Nagatani, W. R. Harris, and J. W. Olness, Phys. Rev. C **3**, 2198 (1971).
[5] D. J. Millener, J. W. Olness, E. K. Warburton, and S. S. Hanna, Phys. Rev. C **28**, 497 (1983).
[6] E. Kwan, C. Wu, N. Summers, G. Hackman, T. Drake, C. Andreoiu, R. Ashley, G. Ball, P. Bender, A. Boston, H. Boston, A. Chester, A. Close, D. Cline, D. Cross, R. Dunlop, A. Finlay, A. Garnsworthy, A. Hayes, A. Laffoley, T. Nano, P. Navrtil, C. Pearson, J. Pore, S. Quaglioni, C. Svensson, K. Starosta, I. Thompson, P. Voss, S. Williams, and Z. Wang, Phys. Lett. B **732**, 210 (2014).
[7] C. Forssén, P. Navrátil, W. E. Ormand, and E. Caurier, Phys. Rev. C **71**, 044312 (2005).
[8] S. Quaglioni and P. Navrátil, Phys. Rev. Lett. **101**, 092501 (2008).
[9] S. Quaglioni and P. Navrátil, Phys. Rev. C **79**, 044606 (2009).
[10] A. Calci and R. Roth, Phys. Rev. C **94**, 014322 (2016).
[11] S. Baroni, P. Navrátil, and S. Quaglioni, Phys. Rev. Lett. **110**, 022505 (2013).
[12] S. Baroni, P. Navrátil, and S. Quaglioni, Phys. Rev. C **87**, 034326 (2013).
[13] P. Navrátil, S. Quaglioni, G. Hupin, C. Romero-Redondo, and A. Calci, Phys. Scr. **91**, 053002 (2016).
[14] S. Weinberg, Physica A: Statistical Mechanics and its Applications **96**, 327 (1979).
[15] S. Weinberg, Phys. Lett. B **251**, 288 (1990).
[16] S. Weinberg, Nucl. Phys. B **363**, 3 (1991).
[17] C. Ordóñez, L. Ray, and U. van Kolck, Phys. Rev. Lett. **72**, 1982 (1994).
[18] U. van Kolck, Phys. Rev. C **49**, 2932 (1994).
[19] E. Epelbaum, A. Nogga, W. Glöckle, H. Kamada, U.-G. Meißner, and H. Witała, Phys. Rev. C **66**, 064001 (2002).
[20] E. Epelbaum, Prog. Part. Nucl. **57**, 654 (2006).
[21] R. Machleidt and D. R. Entem, Phys. Rep. **503**, 1 (2011).
[22] P. Navrátil, Few Body Syst. **41**, 117 (2007).
[23] D. Gazit, S. Quaglioni, and P. Navrátil, Phys. Rev. Lett. **103**, 102502 (2009).
[24] R. Roth, A. Calci, J. Langhammer, and S. Binder, Phys. Rev. C **90**, 024325 (2014).
[25] R. Roth, S. Binder, K. Vobig, A. Calci, J. Langhammer, and P. Navrátil, Phys. Rev. Lett. **109**, 052501 (2012).
[26] A. Ekström, G. R. Jansen, K. A. Wendt, G. Hagen, T. Papenbrock, B. D. Carlsson, C. Forssén, M. Hjorth-Jensen, P. Navrátil, and W. Nazarewicz, Phys. Rev. C **91**, 051301(R) (2015).
[27] G. Hagen, A. Ekstrom, C. Forssen, G. R. Jansen, W. Nazarewicz, T. Papenbrock, K. A. Wendt, S. Bacca, N. Barnea, B. Carlsson, C. Drischler, K. Hebeler, M. Hjorth-Jensen, M. Miorelli, G. Orlandini, A. Schwenk, and J. Simonis, Nat. Phys. **12**, 186 (2016).
[28] M. Miorelli, S. Bacca, N. Barnea, G. Hagen, G. R. Jansen, G. Orlandini, and T. Papenbrock, (2016), arXiv:1604.05381 [nucl-th].
[29] P. Descouvemont and D. Baye, Reports on Progress in Physics **73**, 036301 (2010).
[30] M. Hesse, J. Roland, and D. Baye, Nucl. Phys. A **709**, 184 (2002).
[31] D. Baye, J. Goldbeter, and J.-M. Sparenberg, Phys. Rev. A **65**, 052710 (2002).
[32] B. I. Schneider, Phys. Rev. A **24**, 1 (1981).
[33] J. Dohet-Eraly, P. Navrátil, S. Quaglioni, W. Horiuchi, G. Hupin, and F. Raimondi, Phys. Lett. B **757**, 430 (2016).
[34] G. Hupin, J. Langhammer, P. Navrátil, S. Quaglioni, A. Calci, and R. Roth, Phys. Rev. C **88**, 054622 (2013).
[35] R. Roth, Phys. Rev. C **79**, 064324 (2009).
[36] R. Roth and P. Navrátil, Phys. Rev. Lett. **99**, 092501 (2007).
[37] F. Raimondi, G. Hupin, P. Navrátil, and S. Quaglioni, Phys. Rev. C **93**, 054606 (2016).
[38] J. Langhammer, P. Navrátil, S. Quaglioni, G. Hupin, A. Calci, and R. Roth, Phys. Rev. C **91**, 021301(R) (2015).
[39] S. Binder, J. Langhammer, A. Calci, and R. Roth, Phys. Lett. B **736**, 119 (2014).
[40] R. Roth, J. Langhammer, S. Binder, and A. Calci, J. Phys.: Conf. Ser. **403**, 012020 (2012).
[41] F. Wegner, Ann. Phys. (Leipzig) **506**, 77 (1994).
[42] S. K. Bogner, R. J. Furnstahl, and R. J. Perry, Phys. Rev. C **75**, 061001(R) (2007).
[43] S. Szpigel and R. J. Perry, in *Quantum Field Theory. A 20th Century Profile*, edited by A. N. Mitra (Hindustan Publishing Co., New Delhi, 2000).
[44] R. Roth, J. Langhammer, A. Calci, S. Binder, and P. Navrátil, Phys. Rev. Lett. **107**, 072501 (2011).
[45] J. Kelley, E. Kwan, J. Purcell, C. Sheu, and H. Weller, Nucl. Phys. A **880**, 88 (2012).

[46] N. Aoi, K. Yoneda, H. Miyatake, H. Ogawa, Y. Yamamoto, E. Ideguchi, T. Kishida, T. Nakamura, M. Notani, H. Sakurai, T. Teranishi, H. Wu, S. Yamamoto, Y. Watanabe, A. Yoshida, and M. Ishihara, Nucl. Phys. A **616**, 181 (1997).
[47] Y. Hirayama, T. Shimoda, H. Izumi, H. Yano, M. Yagi, A. Hatakeyama, C. Levy, K. Jackson, and H. Miyatake, Nucl. Phys. A **738**, 201 (2004).
[48] M. D. Schuster, S. Quaglioni, C. W. Johnson, E. D. Jurgenson, and P. Navrátil, Phys. Rev. C **90**, 011301(R) (2014).
[49] M. D. Schuster, S. Quaglioni, C. W. Johnson, E. D. Jurgenson, and P. Navrátil, Phys. Rev. **C92**, 014320 (2015).
[50] P. Descouvemont, Nucl. Phys. A **615**, 261 (1997).
[51] R. Palit, P. Adrich, T. Aumann, K. Boretzky, B. V. Carlson, D. Cortina, U. Datta Pramanik, T. W. Elze, H. Emling, H. Geissel, M. Hellström, K. L. Jones, J. V. Kratz, R. Kulessa, Y. Leifels, A. Leistenschneider, G. Münzenberg, C. Nociforo, P. Reiter, H. Simon, K. Sümmerer, and W. Walus (LAND/FRS Collaboration), Phys. Rev. C **68**, 034318 (2003).
[52] T. Aumann and T. Nakamura, Phys. Scr. **2013**, 014012 (2013).
[53] T. Nakamura, S. Shimoura, T. Kobayashi, T. Teranishi, K. Abe, N. Aoi, Y. Doki, M. Fujimaki, N. Inabe, N. Iwasa, K. Katori, T. Kubo, H. Okuno, T. Suzuki, I. Tanihata, Y. Watanabe, A. Yoshida, and M. Ishihara, Phys. Lett. B **331**, 296 (1994).
[54] N. Fukuda, T. Nakamura, N. Aoi, N. Imai, M. Ishihara, T. Kobayashi, H. Iwasaki, T. Kubo, A. Mengoni, M. Notani, H. Otsu, H. Sakurai, S. Shimoura, T. Teranishi, Y. X. Watanabe, and K. Yoneda, Phys. Rev. C **70**, 054606 (2004).
[55] A. Kumar, R. Kanungo, A. Calci, P. Navratil et al. in preparation.
[56] E. Gebrerufael, A. Calci, and R. Roth, Phys. Rev. C **93**, 031301 (2016).